Accepted Manuscript

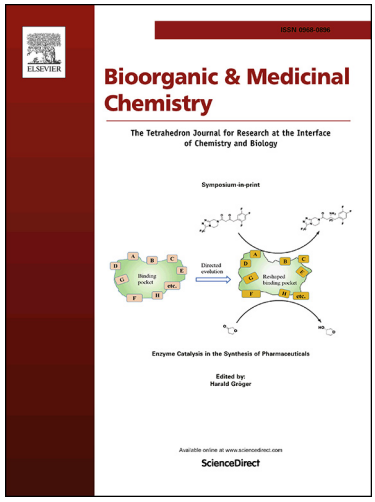

Liposomes modified with double-branched biotin: A novel and effective way to promote breast cancer targeting

Runxin Lu, Lin Zhou, Qiming Yue, Qijun Liu, Xiaojing Cai, Wenjiao Xiao, Li Hai, Li Guo, Yong Wu

PII: S0968-0896(19)30490-0
DOI: https://doi.org/10.1016/j.bmc.2019.05.039
Reference: BMC 14926

To appear in: *Bioorganic & Medicinal Chemistry*

Received Date: 27 March 2019
Revised Date: 23 May 2019
Accepted Date: 27 May 2019

Please cite this article as: Lu, R., Zhou, L., Yue, Q., Liu, Q., Cai, X., Xiao, W., Hai, L., Guo, L., Wu, Y., Liposomes modified with double-branched biotin: A novel and effective way to promote breast cancer targeting, *Bioorganic & Medicinal Chemistry* (2019), doi: https://doi.org/10.1016/j.bmc.2019.05.039

Liposomes modified with double-branched biotin: A novel and effective way to promote breast cancer targeting

Runxin Lu, Lin Zhou, Qiming Yue, Qijun Liu, Xiaojing Cai, Wenjiao Xiao, Li Hai, Li Guo*, Yong Wu*

Key Laboratory of Drug Targeting and Drug Delivery System of Education Ministry, Department of Medicinal Chemistry, West China School of Pharmacy, Sichuan University, Chengdu 610041, P. R. of China

*Corresponding authors. guoli@scu.edu.cn (L. Guo), wyong@scu.edu.cn (Y. Wu).

Abstract Although active targeting liposomes with cancer-specific ligands can bind and internalize into cancer cells, only a few high-efficiency liposomes have been developed so far because traditional single branched ligand modified liposomes generally failed to deliver adequate therapeutic payload. In this paper, we broke the traditional design concept and synthesized the double branched biotin modified cholesterol (Bio_2-Chol) for the first time. On this basis, different biotin density modified liposomes ((Bio-Chol)Lip, $(Bio\text{-}Chol)_2$Lip and (Bio_2-Chol)Lip) were successfully prepared and used as active targeting drug delivery systems for the treatment of breast cancer. The *in vitro* and *in vivo* breast cancer-targeting ability of these liposomes were systemically studied using paclitaxel (PTX) as the model drug. And the uptake mechanism of (Bio_2-Chol)Lip was investigated. The results showed that (Bio_2-Chol)Lip had the best breast cancer-targeting ability compared with naked paclitaxel, unmodified Lip, (Bio-Chol)Lip and $(Bio\text{-}Chol)_2$Lip. In particular, the relative uptake efficiency (RE) and concentration efficiency (CE) of (Bio_2-Chol)Lip were respectively enhanced by 5.61- and 5.06-fold compared to that of naked paclitaxel. Both distribution data and pharmacokinetic parameters suggested that the double branched biotin modified liposome ((Bio_2-Chol)Lip) is a very promising drug delivery carrier for breast cancer.

Keywords: Biotin; Active targeting; Breast tumor; Drug delivery; Liposome

1. Introduction

Breast cancer is the most common type of cancer in women and is the second leading cause of cancer-related deaths worldwide [1]. According to report of the World Health Organization (WHO), 17.5 million breast cancer-related deaths can be expected per year, by 2050 [2]. Currently, comprehensive treatments for breast cancer include surgery, radiotherapy, immunotherapy and chemotherapy [3]. Among these treatments, chemotherapy plays an crucial role in improving the survival rate of breast cancer patients. However, its clinical applications are restricted largely by the high toxicity and non-selectivity [4]. Therefore, considerable attention has been focused on

the modification of classic chemotherapy drugs and the exploitation of new drug delivery systems [5-8].

Tumor-specific active targeting drug delivery system has been widely noted due to its great potential which permits encapsulated chemotherapy drugs to be distributed less in the normal tissue and more in the tumor site. Liposome-based drug delivery systems have attracted considerable attention because of its outstanding merits of their biodegradable, non-toxic and biocompatible features [9-11]. Therefore, the use of targeted liposomes to encapsulate chemotherapy drugs has become an international research hotspot and main development direction in the treatment of breast cancer.

The intense metabolic activity of cancer cell arises from their rapid growth and is accompanied by the intense consumption of essential vitamins [12]. The receptors involved in vitamin internalization are over-expressed on the surface of cancer cells to maintain extensive vitamin uptake and may serve as useful tumor-specific targets for liposomes [12]. Therefore, using vitamin modified liposomes as carriers of chemotherapy drugs recently represent an attractive and valuable strategy for the treatment of cancer. Interestingly, among vitamins, biotin seems to be the most promising targeting agent [13-14]. Biotin (vitamin B7, vitamin H), a water-soluble vitamin, plays an essential role in cell proliferation, signal transduction and many other cellular functions [13]. So far, the sodium-dependent multivitamin transporter (SMVT) on the cell surface has been proved as the key transporter for biotin [15]. Importantly, this transporter has been found to be over-expressed in breast cancer cells (such as 4T1 and MCF7) compared to normal cells [16]. Thus, biotinylation is a promising strategy to enhance the binding/affinity of liposomes to breast tumor cells, leading to increasingly curative anti-tumor therapy [17].

Although active targeting liposomes with cancer-specific ligands can bind and internalize into cancer cells, only a few high-efficiency liposomes have been developed so far because traditional single branched ligand modified liposomes generally failed to deliver adequate therapeutic payload [18]. Simultaneously, treatment with these liposomes is likely to lead to the development of drug-resistant cancers. The same problem exists in single branched biotin modified active targeting drug delivery systems currently used to cure breast cancer. Therefore, we want to develop a novel active targeting liposome which can deliver more drugs into the breast cancer cells than traditional single branched biotin modified liposomes.

We assumed that increasing the density of biotin on the surface of liposomes would increase SMVT-mediated recognition and transshipment. There are two methods to achieve this goal. The one is to simply increase the dosage of single branched biotin modified cholesterol in the preparation of liposomes, and the other is to alter the biotin amount attached to a single cholesterol, keeping the dosage of biotin modified cholesterol unchanged.

In the past decades, several radioactively labeled bis-biotin complexes had been developed to increase the

effects of radiotherapy [19]. Besides, Lo and his co-workers successfully prepared luminescent bis-biotin complexes as the signal amplifiers for heterogeneous recognition assay [20]. Inspired by these literatures, we designed and synthesized the single branched biotin modified cholesterol (Bio-Chol) and double branched biotin modified cholesterol (Bio_2-Chol) for the first time. Liposomes ((Bio-Chol)Lip, $(Bio\text{-}Chol)_2$Lip and (Bio_2-Chol)Lip) modified with different biotin density were prepared to investigate the effect of biotin density on uptake of breast cancer cells (**Fig. 1**). Thereinto, $(Bio\text{-}Chol)_2$Lip had twice single branched biotin modified cholesterol compared with (Bio-Chol)Lip, and (Bio_2-Chol)Lip had the double branched biotin modified cholesterol keeping the dosage of biotin modified cholesterol unchanged.

We want to know whether the drug delivery capacity of $(Bio\text{-}Chol)_2$Lip and (Bio_2-Chol)Lip is twice that of (Bio-Chol)Lip when the density of biotin on the surface of liposomes is doubled. In addition, when the dosage of biotin is kept constant, whether the double branched biotin modified lipsome (Bio_2-Chol)Lip has a stronger drug delivery ability than $(Bio\text{-}Chol)_2$Lip. In order to improve the reliability of results, unmodified liposome was also prepared for contrastive study. The cellular uptake efficiency, *in vivo* breast cancer targeting properties and therapeutic efficacy of these paclitaxel (PTX) loaded liposomes were studied systemically. In addition, the uptake mechanism of (Bio_2-Chol)Lip was investigated.

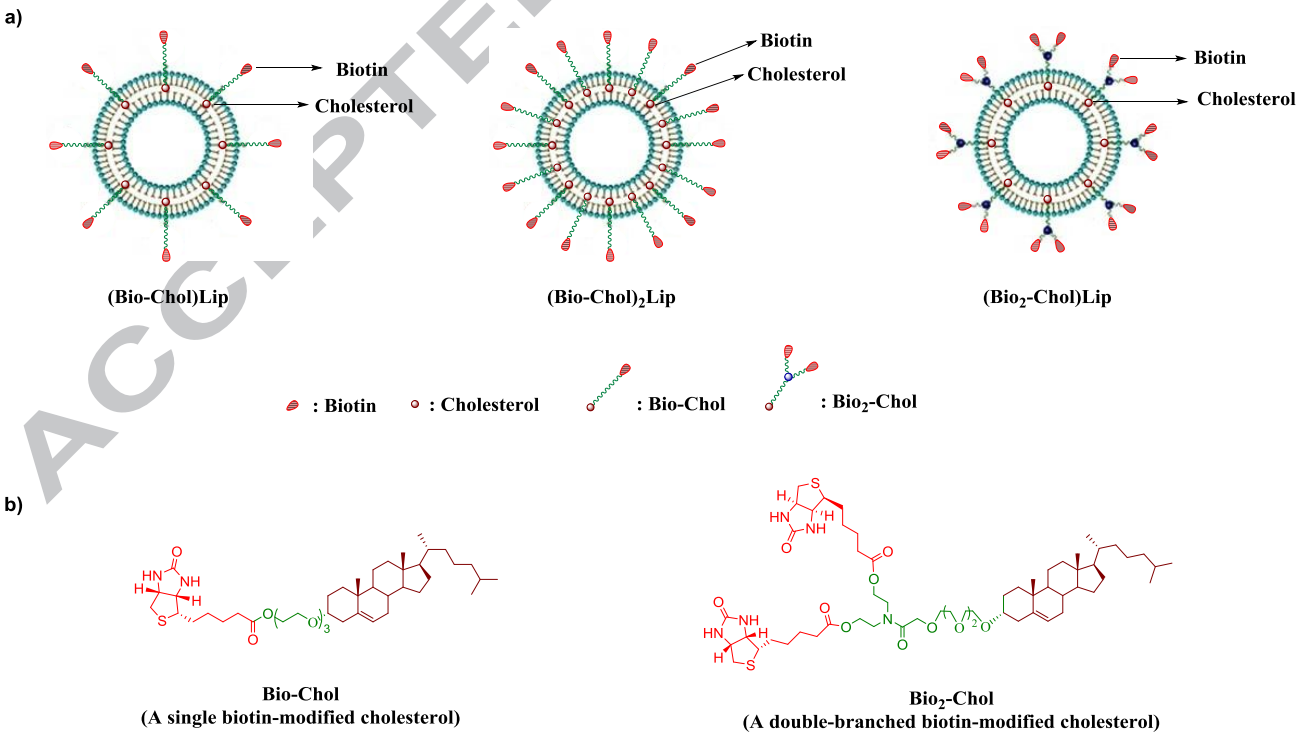

Figure 1. Schematic diagrams of (Bio-Chol)Lip, $(Bio\text{-}Chol)_2$Lip, (Bio_2-Chol)Lip, Bio-Chol and Bio_2-Chol.

2. Materials and methods

2.1. Materials

All liquid reagents were distilled before use. All unspecified reagents were from commercial resources. TLC was performed using precoated silica gel GF254 (0.2 mm), while column chromatography was performed using silica gel (100-200 mesh). ^{1}H NMR spectra was taken on a Varian INOVA 400 (Varian, Palo Alto, CA, USA) using $CDCl_3$, d_6-DMSO and D_2O as solvents. Chemical shifts are expressed in δ (ppm), with tetramethylsilane (TMS) functioning as the internal reference, and coupling constants (J) were expressed in Hz. Mass spectra were recorded on an Agilent 1946B ESI-MS instrument (Agilent, Palo Alto, CA, USA). Paclitaxel and docetaxel were obtained from National Institute for Food and Drug Control. Soybean phospholipids (SPC) was purchased from Kelong Chemical (Chengdu, China). Cholesterol (Chol) was purchased from Bio Life Science & Technology Co., Ltd (Shanghai, China). D-(+)-Biotin was purchased from shanghai darui fine chemical Co., Ltd (Shanghai, China). 1,2-dioleoyl-snglycero-3-phosphoethanolamine-N-(carboxyfluorescein) (CFPE) was purchased from Avanti Polar Lipids (USA). 4'-6-Diamidino-2-phenylindole (DAPI) and 3-(4,5-Dimethylthiazol-2-yl)-2,5-diphenyltetrazolium bromide (MTT) were purchased from Beyotime Institute Biotechnology (Haimen, China). Sodium azide, amiloride, chlorpromazine, filipin, biotin-NHS, valeric acid, ascorbic acid, pantothenic acid and thiamine were obtained from Sigma-Aldrich (St. Louis, MO, USA). 4-chlorobenzenesulfonate salt (DiD) was purchased from Biotium (USA). Annexin V-FITC/PI apoptosis detection kit was obtained from KeyGEN Biotech (China). A Diamonsil column (200 × 4.6 mm, 5 mm) was used. A LC-10A liquid chromatographic system (Shimadzu) and a reverse-phase HPLC column (ODS-C18 column, 4.6mm × 200 mm, 5 mm, SinoChrom, Dalian, China) were used.

*2.2. Synthesis of compounds **2-5***

The synthesis of compounds **2-5** were reported in our previous work [21].

*2.3. Synthesis of compound **6***

To a solution of compound **5** (4.00 g, 6.93 mmol) in CH_2Cl_2 (30 mL) was added NMM (0.84 mL, 7.63 mmol) and IBCF (0.96 mL, 7.63 mmol), and the reaction was stirred at -10 ^{o}C for 30 min. Then, diethanol amine (1.09 g, 10.40 mmol) in CH_2Cl_2 (15 mL) was added slowly. After stirring for another 6h at room temperature, the mixture was washed with 1 mol/L HCl and saturated NaCl solution. The organic layer was dried over anhydrous Na_2SO_4, and concentrated in vacuo. The residue was purified by flash column chromatography to afford compound **6** (4.09 g, 89%) as a pale yellow oil. ^{1}H NMR (400 MHz, $CDCl_3$, ppm) δ: 0.67 (s, 3H), 0.86 (d, 6H, J = 6.4 Hz), 0.91 (d, 3H, J = 6.4 Hz), 0.99 (s, 3H), 1.01-2.38 (remaining cholesterol protons), 3.14-3.21 (m, 1H), 3.50-3.85 (m, 20H), 4.28 (s,

2H), 5.34 (d, 1H, *J* = 4.8 Hz). HRMS (ESI) Calcd. for $C_{39}H_{69}NO_7Na$ $[M + Na]^+$ 686.4966, found 686.4968.

2.4. Synthesis of ligand Bio$_2$-Chol

To a solution of D-(+)-Biotin (147 mg, 0.604 mmol) in CH_2Cl_2 (10 mL) and N,N-Dimethylformamide (5 mL) was added EDCI (145 mg, 0.755 mmol), DMAP (92 mg, 0.755 mmol) and DIPEA (156 μL, 1.21 mmol), and the reaction was stirred at room temperature for 30 min. Then compound **6** (100 mg, 0.151 mmol) in CH_2Cl_2 (5 mL) was added slowly. After stirring for another 14h at room temperature, the mixture was washed with 1 mol/L HCl and saturated NaCl solution. The organic layer was dried over anhydrous Na_2SO_4, and concentrated in vacuo. The residue was purified by flash column chromatography to afford ligand Bio$_2$-Chol (110 mg, 65%) as a white vesicular solid. ^{1}H NMR (400 MHz, $CDCl_3$, ppm) δ: 0.67(s, 3H), 0.86 (d, 6H, *J* = 6.4 Hz), 0.91 (d, 3H, *J* = 6.4 Hz), 0.99 (s, 3H), 1.02-2.23 (remaining cholesterol & biotin protons), 2.34 (s, 4H), 2.75-2.78 (m, 2H), 2.90-2.93 (m, 2H), 3.15 (s, 3H), 3.63-3.70 (m, 16H), 4.25-4.34 (m, 8H), 4.53 (s, 2H), 5.33 (s, 1H). HRMS (ESI) Calcd. for $C_{59}H_{97}N_5O_{11}S_2Na$ $[M + Na]^+$ 1138.6518, found 1138.6520.

2.5. Synthesis of ligand Bio-Chol

To a solution of D-(+)-Biotin (57 mg, 0.23 mmol) in CH_2Cl_2 (5 mL) and N,N-Dimethylformamide (2 mL) was added EDCI (56 mg, 0.29 mmol), DMAP (35 mg, 0.29 mmol) and N,N-Diisopropylethylamine (DIPEA) (75 mg, 0.58 mmol), and the reaction was stirred at room temperature for 30 min. Then compound **3** (100 mg, 0.19 mmol) in CH_2Cl_2 (5 mL) was added slowly. After stirring for another 14h at room temperature, the mixture was washed with 1 mol/L HCl and saturated NaCl solution. The organic layer was dried over anhydrous Na_2SO_4, and concentrated in vacuo. The residue was purified by flash column chromatography to afford ligand Bio-Chol (110 mg, 76%) as a white vesicular solid. ^{1}H NMR (400 MHz, $CDCl_3$, ppm) *δ*: 0.69 (s, 3H), 0.88 (d, 6H, *J* = 6.4 Hz), 0.93 (d, 3H, *J* = 7.2 Hz), 1.01 (s, 3H), 0.88-2.04 (remaining cholesterol & biotin protons), 2.19-2.25 (m, 1H), 2.36-2.41 (m, 3H), 2.82 (m, 2H), 3.16-3.24 (m, 2H), 3.65-3.73 (m, 10H), 4.22-4.30 (m, 2H), 4.41 (s, 1H), 4.61 (s, 1H), 5.36 (s, 1H). HRMS (ESI) Calcd. for $C_{43}H_{72}N_2O_6SNa$ $[M+ Na]^+$ 767.5003, found 767.5005.

2.6. Preparation and characterization of liposomes

Liposomes were prepared by the thin film hydration method described previously [22]. Lipid composition of the prepared liposomes were as follows: (1) unmodified liposomes (Lip): SPC/cholesterol (molar ratio = 62: 33); (2) ligand Bio$_2$-Chol modified liposomes ((Bio$_2$-Chol)Lip): SPC/cholesterol/Bio$_2$-Chol (molar ratio = 62: 33: 3); (3) ligand Bio-Chol modified liposomes ((Bio-Chol)Lip): SPC/cholesterol/Bio-Chol (molar ratio = 62: 33: 3); (4)

ligand Bio-Chol modified liposomes ((Bio-Chol)$_2$Lip): SPC/cholesterol/Bio-Chol (molar ratio = 62: 33: 6). All lipid materials were dissolved in the mixture solvent chloroform/methanol (v/v = 2:1), and then the organic solvent was removed by rotary evaporation to form a lipid film. After kept in vacuum overnight, the obtained film was hydrated in PBS (pH = 7.4) for 0.5h at 20 ^{o}C. Then it was further intermittently sonicated by a probe sonicator at 80 W for 90 s to form liposomes.

Free PTX was prepared as follows: PTX was dissolved in a mixture of ethanol-Cremophor ELP35 with a volume ratio of 1:1. PTX-loaded liposomes were prepared with PTX added to the lipid organic solution prior to the solvent evaporation. The entrapment efficiency (EE) of PTX was determined by high performance liquid chromatography (HPLC, Agilent 1200 series, Palo Alto, CA). Likewise, CFPE-labelled or DiD-loaded liposomes were prepared by adding appropriate amount of CFPE or DiD to the solution before the solvent evaporation.

The mean size and zeta potential of Lip, (Bio-Chol)Lip, (Bio-Chol)$_2$Lip and (Bio$_2$-Chol)Lip were detected by Malvern Zetasizer Nano ZS90 instrument (Malvern Instruments Ltd., U.K).

2.7. In vitro drug release study

In order to investigate the PTX release behavior of all liposomes, an *in vitro* drug release assay was conducted using dialysis method [23]. Each PTX-loaded liposome (0.8 mL) or free PTX were placed into dialysis tubes (MWCO = 8000-14000 Da) and tightly sealed. Then the dialysis tubes were placed into 40 mL PBS containing 0.1% (v/v) Tween 80 and incubated under 37 °C for 48h with gentle oscillating at 45 rpm. At predetermined time points (0h, 1h, 2h, 4h, 8h, 12h, 24h and 48h), 0.1 mL release medium was sampled and replaced with equal volume of fresh release medium. Then the samples were diluted with acetonitrile and the concentrations of PTX were determined at the wavelength of 227 nm by HPLC.

2.8. In vitro stability of liposomes in serum

Turbidity variations were measured to demonstrate the serum stability of liposomes in the presence of fetal bovine serum (FBS). Briefly, liposomes were mixed with equal volume of FBS under 37 °C with moderate shaking at 45 rpm. At predetermined time points (0h, 1h, 2h, 4h, 8h, 12h, 24h and 48h), 200 μL of the sample was pipetted out and onto a 96-well plate to measure the transmittance of the mixture at 750 nm by a microplate reader (Thermo Scientific Varioskan Flash, USA).

2.9. Hemolysis assays

To evaluate the safety of ligand-modified liposomes during body circulation, hemolysis assay was performed.

Fresh mice blood was collected in tubes containing heparin sodium. The red blood cells (RBCs) were separated and collected by centrifugation at 5×10^3 rpm for 10 min, and washed several times with PBS until the supernatant became colorless. After the last wash, the RBCs were diluted with PBS to a concentration of 2% (v/v). Various concentrations of liposomes were incubated with equal volume of 2% RBCs solutions for 1h at 37 ^{o}C with moderate shaking at 45 rpm, followed by centrifugation at 1×10^4 rpm for 10 min. Absorbance of hemoglobin was measured using a microplate reader (Thermo Scientific Varioskan Flash) at 540 nm.

RBC hemolysates in PBS solutions and in 1% Triton X-100 were used as negative and positive controls, respectively.

The percent hemolysis = $\frac{A_{Sample}-A_{Negative}}{A_{Postive}-A_{Negative}} \times 100\%$, where A is the absorbance of hemoglobin.

2.10. Cell line and Cell culture

SMVT over-expressed cells (4T1 and MCF7 cells) and SMVT negative expressed B16 cell [16] were used in this study. MCF-7 cells (Human breast cancer cell line), 4T1 cells (Mouse breast cancer cell line) and B16 cells (Mouse skin melanoma cell line) were cultured in Dulbecco's Modified Eagles Medium (DMEM) and RPMI 1640 supplemented with 10% FBS, 100 U/mL streptomycin, and 100 U/mL penicillin at 37 °C in a 5% CO_2 humidified environment incubator (Thermo Scientific, USA).

2.11. In vitro cellular uptake study

4T1 cells, MCF-7 cells and negative cell line B16 cells were seeded in 12-well plates at a density of 3×10^5 cells/well and cultured for 24h at 37 ^{o}C. Different CFPE-labeled liposomes were added into each well with a final concentration of CFPE at 2 μg/mL. After cultured for 4h at 37 ^{o}C, the cells were washed three times with cold PBS, trypsinized, and finally resuspended in 0.3 mL PBS. Then, the fluorescent intensity of cells treated with different liposomes was measured by a flow cytometer (BD FACSCelesta, BD, USA).

For qualitative experiments, 4T1 cells, MCF-7 cells and B16 cells were plated onto a 6-well plate containing cover glass at a density of 3×10^5 cells/well and cultured for 24h at 37 ^{o}C. CFPE-labeled liposomes were added into each well with a final concentration of CFPE at 2 μg/mL and allowed for further co-incubation for 4h. Following that, the cells were rinsed with cold PBS for three times and fixed with 4% paraformaldehyde for 30 min at room temperature, and then cell nuclei were stained with DAPI (5 μg/mL) for 5 min. Finally, the samples were imaged using Laser Scanning Confocal Microscope (CLSM) (LSM800, Carl Zeiss AG, Germany).

2.12. Uptake mechanism study

In order to study the uptake mechanism of how (Bio_2-Chol)Lip was delivered into cells. Endocytosis inhibition assay and SMVT transport verification experiment were carried out. For Endocytosis inhibition assay, 4T1 cells and MCF-7 cells were preincubated with various endocytosis inhibitors, such as sodium azide (50 mM), amiloride (5 mM), chlorpromazine (5 μg/ml) and filipin (3.5 μg/ml), meanwhile the effect of temperature (both 37 °C and 4 °C) were also studied.

SMVT is a Na^+-dependent multivitamin transporter that mediates cellular uptake of biotin, pantothenic acid, and lipoic acid [15]. Biotin transported by SMVT appears to be time-, concentration-, sodium ion-dependent but independent of chloride ions. It was also significantly inhibited in the presence of biotin and other SMVT substrates, such as pantothenic acid. The carboxyl group was considered to be a key feature for interaction with SMVT, structurally unrelated vitamins had no influence in SMVT transporting [15].

Therefore, to confirm the involvement of SMVT, time-, concentration-, ion dependence assays and substrate specificity test were executed. Uptake of (Bio_2-Chol)Lip on 4T1, MCF7 cells was assessed at different time and various concentrations. To investigate the effect of sodium ions on the uptake of (Bio_2-Chol)Lip, equimolar quantities of choline chloride and dipotassium phosphate were added to replace sodium chloride and sodium phosphate in the buffer, respectively. In a similar way to delineate the effect of chloride ions, sodium, potassium and calcium chlorides in the buffer were replaced with equimolar quantities of sodium phosphate, potassium phosphate and calcium acetate respectively. Structural requirements of the carrier mediated system were delineated by performing uptake experiments in the presence of competitive inhibitors such as unlabeled biotin (10 mM), pantothenic acid (10 mM). Further we examined the influence of free carboxylic group (COOH) on biotin uptake by incubating cells with structural analogs such as valeric acid (10mM) which possess a free carboxylic acid group, and biotin-NHS (10 mM) which devoid free carboxylic group. Similar study was performed in the presence of other vitamins such as ascorbic acid (10 mM) and thiamine (10 mM) to examine the effect of structurally unrelated vitamins on uptake of biotin in 4T1 cells and MCF-7 cells.

Briefly, the cells were preincubated with different inhibitors for 30 min at 37 °C, then the inhibitors were withdrawn from the wells and CFPE-labeled (Bio_2-Chol)Lip was added. After cultured for 4h at 37 ^oC, the cells were treated as described in *2.11.* and the fluorescent intensity was measured by a flow cytomete (BD FACSCelesta, BD, USA).

2.13. In vitro cytotoxicity study

2.13.1. MTT assay

The cytotoxicity of PTX-loaded liposomes and free PTX against 4T1 cells and MCF-7 cells were measured with 3-(4,5-dimethyl-2-thiazolyl)-2,5-diphenyl-2-H-tetrazoliumbromide (MTT) assay. Generally, the cells were seeded in a 96-well plate at a density of 5×10^3 cells/well and cultured for 24h at 37 ^{o}C. PTX-loaded liposomes and free PTX were diluted to predetermined concentrations with medium, and added into each well for 48h incubation. The final concentrations of PTX were in the range of 0.01-20 μg/mL.

Blank liposomes and the solvent of free PTX (ethanol-cremophor ELP 35 mixture, v/v =1: 1) were added at the same concentration of PTX-loaded liposomes as well.

Then, 20 μL MTT solutions (5.0 mg/mL in PBS) was added into each well and incubated for another 4h at 37 °C. After removal of the culture medium, cells were dissolved by 150 μL dimethyl sulfoxide. The absorbance was measured at 490 nm wavelength on an automatic microplate spectrophotometer (Thermo Scientific Varioskan Flash, USA). Cell viability (%) was calculated as the following equation: A_{test} / $A_{control}$ × 100%, where A_{test} and $A_{control}$ represented the absorbance of treated cells and control cells, respectively.

2.13.2. Apoptosis assay

The quantitative analysis of cell apoptosis induced by different PTX-loaded liposomes was determined by an Annexin V-FITC/PI apoptosis detection kit, 4T1 cells were treated with PTX-loaded liposomes (PTX concentration is 0.01 μg/ml) for 24h under 37 ^{o}C. Free PTX group was used as control. Cells were harvested, washed three times with cold PBS and resuspended in 500 μL binding buffer. Then 5 μL Annexin V-FITC and 5μL PI were added and incubated with the cells for 15 min in the dark. Finally, the stained cells were analyzed by a flow cytometer (BD FACSCelesta, BD, USA).

2.14. Distribution in vivo and pharmacokinetic studies in mice

2.14.1. Animals

Female BALB/c mice (5–6 weeks, 18–22 g) were purchased from Dashuo Biotechnology Co., Ltd. (Chengdu, China), and all animals experiments were performed according to the experimental guidelines of the Animal Experimentation Ethics Committee of Sichuan University. Throughout the experiments, the animals were handled according to the requirements of the National Act on the use of experimental animals (China).

2.14.2. Tumor model

Female BALB/c mice were anesthetized, and 4T1 cells (1×10^7 cells/mL, 100 μL) were slowly injected into

the right upper thigh subcutaneous region. Tumors were allowed to grow to an average volume of 70-100 mm^3 (tumor volume = length × $width^2$ × 0.52) before the *in vivo* bio-distribution and imaging.

2.14.3. Sample preparation

Blood was collected from the eye socket of mice into tubes containing heparin sodium, and centrifuged at 5500 rpm for 10 min. The supernatant was collected as plasma sample.

In addition, the organs (heart, liver, spleen, lung and kidney) and tumor tissues were removed after excretion of blood by cardiac perfusion with saline, and washed twice, then flushed with saline for three times to remove the blood remained, finally, the organs and tumor tissues were rolled over on the filter paper carefully to remove the main vessel. All the tissues were homogenized with triple amount of saline.

An aliquot of 30 μL or 10 μL of internal standard (docetaxel, 100 μg/mL) was added into 100 μL plasma or 100 μL tissues homogenate, and extracted with 400 μL ether. The mixture was vortexed for 5 min, and centrifuged at 10000 rpm for 15 min. The supernatant was transferred to another centrifuge tube, and dried under air stream at room temperature. The dry residue was reconstituted with 100 μL of methanol. The solution was centrifuged at 10000 rpm for 15 min, and then 20 μL of the supernatant was injected into the HPLC system for analysis.

2.14.4. In vivo bio-distribution

Tumor targeting capability of free PTX, PTX-Lip, PTX-(Bio-Chol)Lip, PTX-$(Bio\text{-}Chol)_2$Lip and PTX-(Bio_2-Chol)Lip for intravenous injection was investigated in subcutaneous 4T1 model. The xenograft 4T1-breast tumor bearing mice were randomly divided into groups (3 mice each) for the four types of liposomes and PTX. PTX-Lip, PTX-(Bio-Chol)Lip, PTX-$(Bio\text{-}Chol)_2$Lip, PTX-(Bio_2-Chol)Lip and free PTX were given to the mice *via* the tail vein and each was equivalent to the administration dose of PTX of 10 mg/kg. At 5 min, 15 min, 30 min, 60 min, 120 min, 240 min, 480 min, 720 min and 1440 min after injection, blood samples were collected from the eye socket of mice, and placed in tubes containing heparin sodium. Likewise, at the predetermined time points after injection, the organs and tumor tissues were removed after excretion of blood by cardiac perfusion with saline. All the tissues were prepared as described in *2.14.3*. The concentration of PTX was analyzed by HPLC.

2.14.5. In vivo imaging

The active targeting ability of Lip, (Bio-Chol)Lip, $(Bio\text{-}Chol)_2$Lip, (Bio_2-Chol)Lip was studied in 4T1-breast tumor bearing BALB/c mice. The 4T1-breast tumor bearing BALB/c mice were randomly divided into four groups (4 each group) and were intravenously injected *via* the caudal vein with DiD-Lip, DiD-(Bio-Chol)Lip,

DiD-(Bio-Chol)$_2$Lip and DiD-(Bio$_2$-Chol)Lip at a dose of 200 μg DiD/kg. The DiD fluorescence signal (Ex 620 nm, Em 670 nm) was imaged by the IVIS Lumina Series III imaging system (Perkin-Elmer, USA) at 1h, 2h, 8h and 24h after injection.

2.15. Statistical analysis

The area under the concentration-time profile (AUC_{0-t}), maximal concentration (C_{max}), and mean residence times (MRT) were calculated by Data and max Statistics (DAS 2.0, Shanghai, China). The relative uptake efficiency (RE) and concentration efficiency (CE) were calculated to evaluate the breast tumor targeting capability of liposome. The value of RE and CE were defined as follows:

$RE = (AUC_{0-t})_L / (AUC_{0-t})_P$

$CE = (C_{max})_L / (C_{max})_P$,

where L and P represented the liposomes loading PTX and free PTX, respectively.

The results were expressed as means ± standard deviations (s.d.) of the mean. Data comparison between two different groups were analyzed using an F-test with subsequent T-tests (equal variance). Statistical comparisons were performed by one-way ANOVA for multiple groups. Significant differences between or among groups were indicated by *p < 0.05, **p < 0.01 and ***p < 0.001, respectively.

3. Results and discussion

3.1. Synthesis of ligand Bio$_2$-Chol

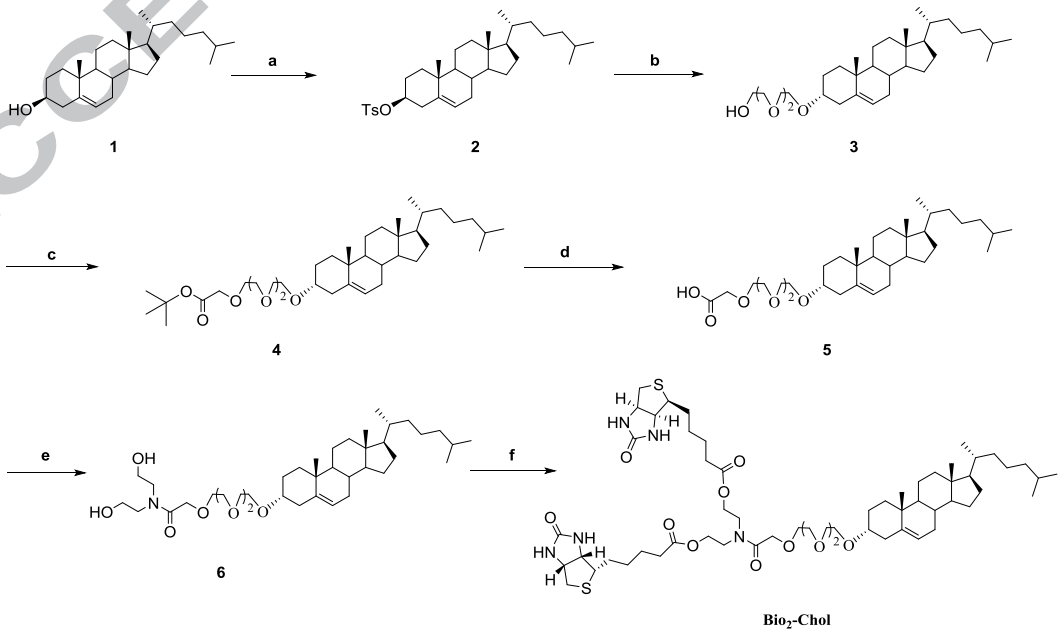

Scheme 1. The synthetic route of ligand Bio_2-Chol. Reagents and conditions: (a) TsCl, pyridine, 50 ^oC, 5h. (b) Triethylene glycol, dioxane, reflux, 6h. (c) *t*-butyl bromoacetate, *n*-$Bu_4N^+HSO_4^-$, 50% NaOH, toluene, r.t., 16h. (d) TsOH, toluene, reflux, 8h. (e) Diethanol amine, IBCF, NMM, CH_2Cl_2, -10 ^oC, r.t., 5h; (f) D-(+)-Biotin, EDCI, DMAP, DIPEA, CH_2Cl_2, r.t., 12h.

The synthetic route of ligand Bio_2-Chol was illustrated in Scheme 1. Firstly, compound **5** was synthesized from cholesterol (**1**) in four steps, which was then conjugated with diethanol amine in the presence of isobutyl chloroformate (IBCF) and *N*-methyl morpholine (NMM) to obtain compound **6**. Finally, compound **6** reacted with D-(+)-biotin to give the target compound Bio_2-Chol under the condensation condition. The target compound and important intermediates were characterized by ^1H NMR and mass spectra.

3.2. Synthesis of ligand Bio-Chol

Scheme 2 showed the synthetic route of ligand Bio-Chol. Similarly, compound **3** was synthesized from cholesterol (**1**) in two steps, then was conjugated with D-(+)-biotin in the presence of EDCI and DMAP to obtain ligand Bio-Chol.

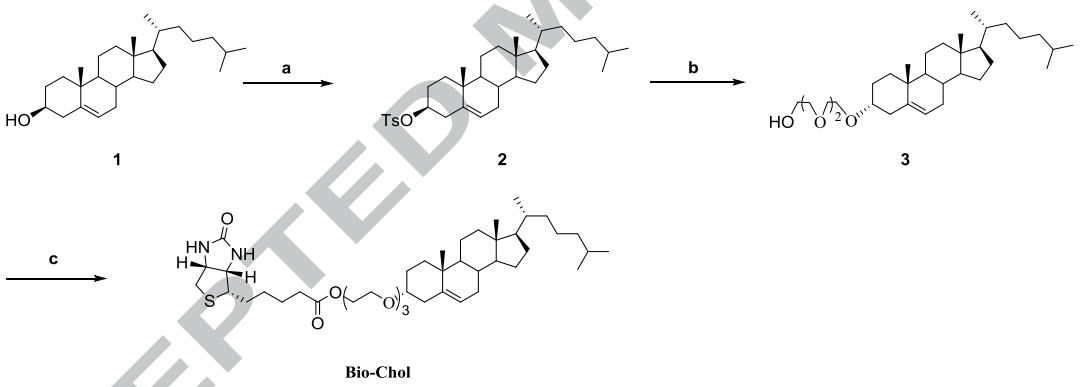

Scheme 2 .The synthetic route of ligand Bio-Chol. Reagents and conditions: (a) TsCl, pyridine, 50 ^oC, 5h. (b) Triethylene glycol, dioxane, reflux, 6h. (c) D-(+)-Biotin, EDCI, DMAP, DIPEA, CH_2Cl_2, r.t., 12h.

3.3. Characterization of liposomes

Proper size, uniform distribution and zeta potential of nanoparticles are crucial to cellular uptake efficiency, *in vivo* bio-distribution and so on [25]. The mean diameter, encapsulation efficiency and zeta potential of these liposomes were exhibited in Table 1. Dynamic light scattering (DLS) showed the average particle sizes of these liposomes were about 110 nm with a polydispersity index (PDI) less than 0.2. Liposomes are all negatively charged, and their zeta potentials are mainly in the range of -2 to -3 mV.

PTX could be successfully loaded into these liposomes with entrapment efficiency (EE%) above 87%, suggesting that PTX was well loaded, and were suitable for the follow-up *in vitro* and *in vivo* assays (Table 1).

In addition, the PTX-(Bio$_2$-Chol)Lip showed a regular circular shape and a suitable size under the transmission electron microscope (TEM) (**Fig. 2**). The above results indicated that liposomes we prepared could be used for subsequent studies, such as cell uptake, *in vivo* distribution, etc.

Table 1. The composition and characterization of different paclitaxel-loaded liposomes (n = 3, mean ± SD).

Liposomes	Size(nm)	PDI	EE (%)	Zeta potential (mV)
PTX-Lip	103.3 ± 2.1	0.135 ± 0.016	91.23 ± 2.48	-3.06 ± 0.22
PTX-(Bio-Chol)Lip	108.1 ± 1.5	0.147 ± 0.023	87.45 ± 1.36	-3.53 ± 0.17
PTX-(Bio-Chol)$_2$Lip	105.6 ± 2.7	0.121 ± 0.042	87.02 ± 2.06	-2.18 ± 0.32
PTX-(Bio$_2$-Chol)Lip	112.4 ± 2.5	0.119 ± 0.008	88.15 ± 1.64	-2.67 ± 0.18

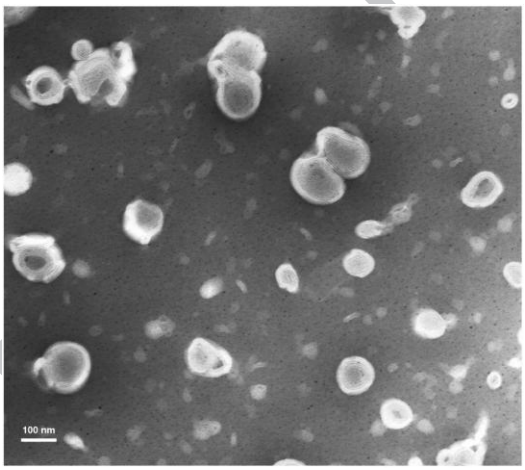

Figure 2. The TEM image of PTX-(Bio$_2$-Chol)Lip.

3.4. In vitro PTX release study

PTX release properties were evaluated in PBS containing 0.1% Tween 80. As shown in **Fig. 3**, free PTX exhibited a rapid release, with more than 80% of the drug released into the medium after 12h incubation. PTX-loaded liposomes achieved sustained release behaviors with cumulative PTX release less than 75% within 48h incubation in PBS. Besides, it was also noted that no significant difference in release properties was observed among PTX-Lip, PTX-(Bio-Chol)Lip, PTX-(Bio-Chol)$_2$Lip and PTX-(Bio$_2$-Chol)Lip, and none of these four kinds of PTX-loaded liposomes displayed a sudden initial release pattern. All the results showed that biotin modification didn't change the release profile of PTX in liposomes.

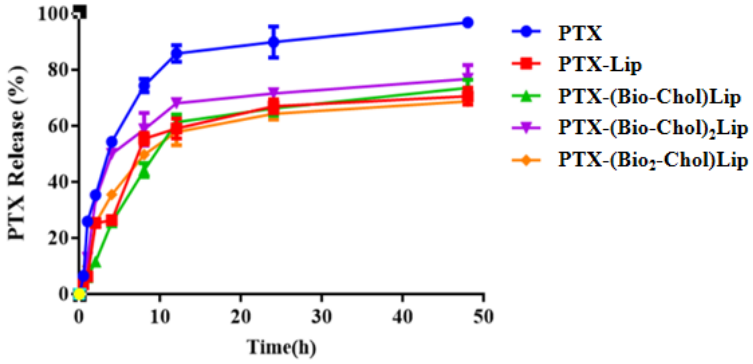

Figure 3. The PTX release profiles of free PTX, PTX-Lip, PTX-(Bio-Chol)Lip, PTX-(Bio-Chol)$_2$Lip and PTX-(Bio$_2$-Chol)Lip in PBS (pH 7.4) containing 0.1% Tween 80 over 48h (n = 3, mean ± SD).

3.5. In vitro stability of liposomes in serum

Liposomal particle stability against physiological condition is prerequisite for the further application *in vivo*, so 50% fetal bovine serum (FBS) was used to mimic the *in vivo* condition. Transmittance variations of different liposomes as important parameters were monitored in our study to explore the serum stability of liposomes. As shown in **Fig. 4**, the transmittance of liposomes were above 90% and showed no detectable change within 48h. The results indicated that liposomes were sufficient to prevent the interaction between liposomes and serum proteins, which was important for obtaining a longer half-life of blood *in vivo* [25].

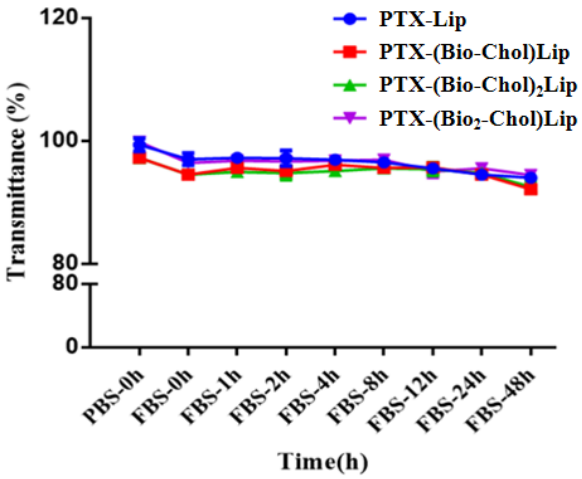

Figure 4. The variations of transmittance of different modified liposomes in 50% FBS (n =3, mean ± SD).

3.6. Hemolysis assays

Hemocompatibility is the key to the application of liposomes *in vivo*. As shown in **Fig. 5**, the hemolysis test

showed that even when the concentration of phospholipids increased to 400 nM, the hemoglobin release of all liposomes did not increase significantly.

PTX-(Bio_2-Chol)Lip did not display concentration-dependent increase in hemolysis as well and less than 10% hemolysis was always regarded as non-toxic [25]. It was reported that cationic delivery vectors could cause cell lysis and hemoglobin release [28]. The result of hemolysis assays was also consistent with the negative potential of biotin-modified liposomes shown in Table 1. In conclusion, all types PTX-loaded liposomes could not interact with negatively charged membrane of the erythrocytes because of electrostatic repulsion of negatively charge, suggesting that PTX-loaded liposomes of biotin modification showed minimal undesirable effects.

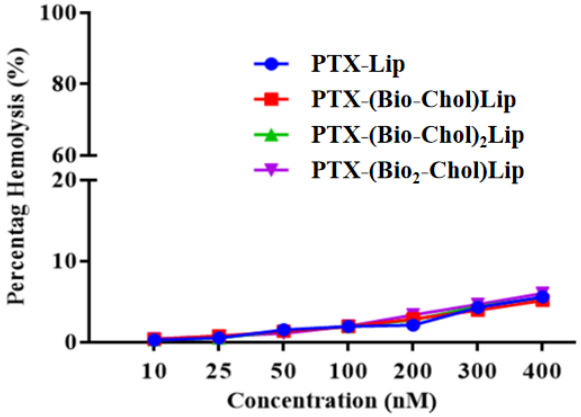

Figure 5. Hemolysis percentage of different liposomes. Values are represented as mean ± SD (*n* =3).

3.7. Cellular uptake study

To demonstrate the preference of biotin-modified liposomes for the breast cancer cells, the cellular uptake of different biotin density modified liposomes was studied and unmodified liposome was used as a negative control. SMVT over-expressed cells (4T1 and MCF7 cells) and SMVT negative expressed cells (B16 cells) were used to investigate the cellular uptake *in vitro*.

As flow cytometry results showed (**Fig. 6A-B**), in SMVT over-expressed cells, liposomes modified with Bio_2-Chol have stronger affinity with the transporters than other types of liposomes. (Bio_2-Chol)Lip displayed more uptake than Lip (3.17-time higher), (Bio-Chol)Lip (2.50-time higher), and (Bio-Chol)$_2$Lip (2.17-time higher) in 4T1 cells. The same trend was observed in MCF7 cells (**Fig. 6B**). In contrast, no significant difference on fluorescence intensity was observed among groups in the SMVT negative expressed cells (B16 cells) (**Fig. 6C**). Notably, similar results were obtained from confocal images (**Fig. 6D-F**).

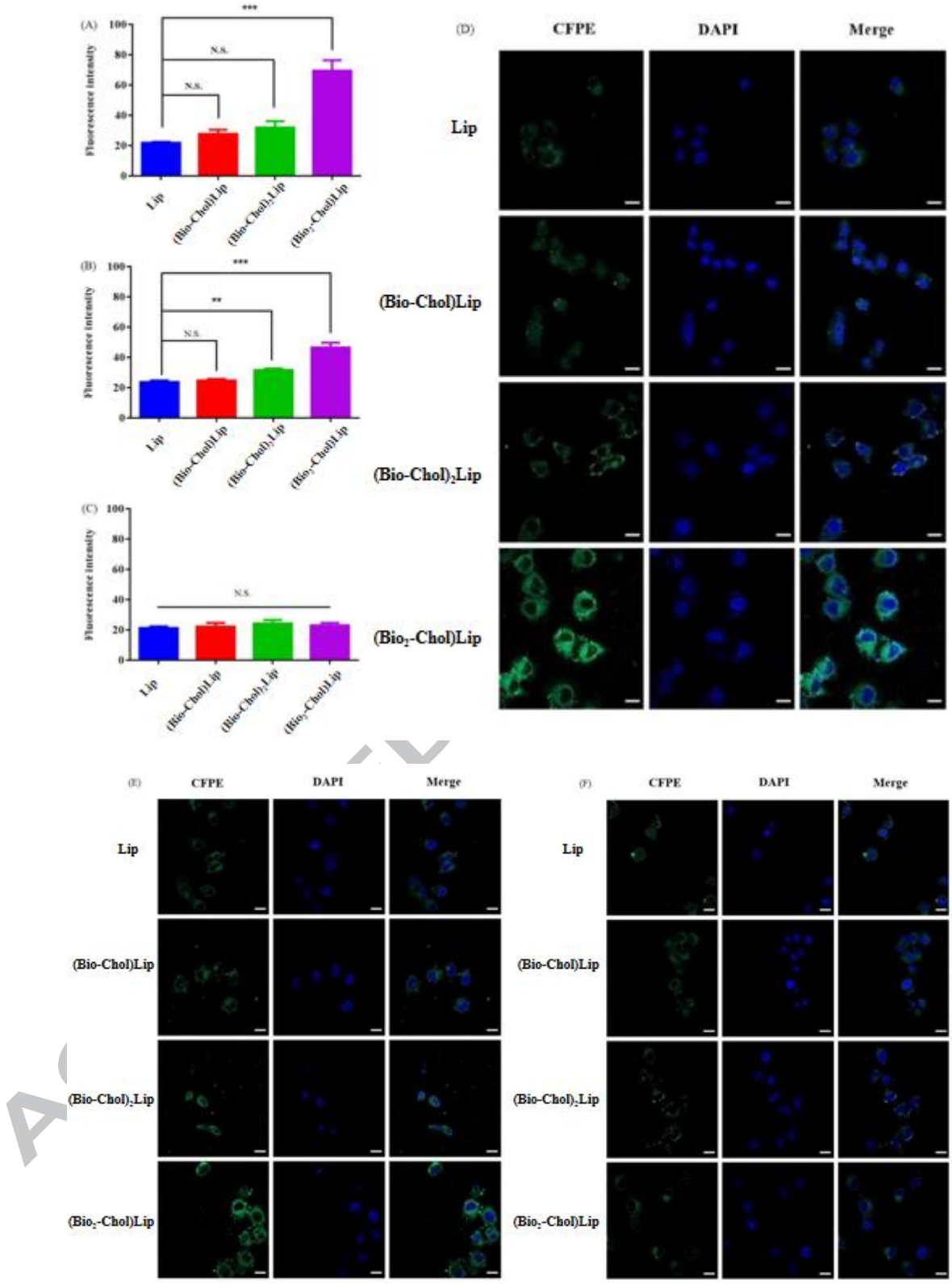

Figure 6. Cellular uptake of CFPE-labeled Lip, (Bio-Chol)Lip, (Bio-Chol)$_2$Lip and (Bio$_2$-Chol)Lip on 4T1 cells, MCF-7 cells and B16 cells were measured. (a) (A), (B), (C) represented cellular uptake of CFPE-labeled liposomes measured by a flow cytometer on 4T1 cells, MCF-7 cells and B16 cells, respectively (mean ± SD, *n* =3). (b) (D), (E), (F) represented qualitative 4h cellular uptake of

CFPE-labeled liposomes determined by CLSM on 4T1 cells, MCF-7 cells and B16 cells, respectively (mean ± SD, *n* =3), green (CFPE-labeled liposomes), blue (DAPI stained nucleus), light blue (colocalized CFPE and DAPI). Scale bars represent 20 μm. *, ** and *** represent $p < 0.05$, $p < 0.01$ and $p < 0.001$ versus Lip group, N. S. indicates none significant difference.

Both flow cytometry and confocal images indicated that (Bio_2-Chol)Lip having a higher cellular internalization in SMVT over-expressed cells but no effect on the uptake of SMVT negative expressed B16 cells. These data suggested that increasing the density of biotin on the surface of liposomes can significantly increase its ability to deliver drugs into breast cancer cells. Furthermore, when the amount of biotin residue on the liposome surface was the same, the liposomes modified by double branched biotin ((Bio_2-Chol)Lip) had better targeting ability for breast cancer than those modified by single biotin ((Bio-Chol)$_2$Lip), especially in 4T1 cells (3.17-time higher than Lip). Above all, (Bio_2-Chol)Lip had the greatest targeting efficacy on breast cancer cells.

3.8. Cellular Uptake mechanism study

The cellular uptake mechanism of (Bio_2-Chol)Lip was also investigated, and a series of endocytosis inhibitors were pre-incubated with 4T1 cells and MCF-7 cells. Chlorpromazine, filipin and amiloride were chosen to block clathrin-mediated endocytosis, caveolin-mediated endocytosis and micropinocytosis respectively [28]. 4°C and NaN_3 (oxidative phosphorylation inhibitor) were selected to study the effect of energy. As the results showed (**Fig. 7A and 7C**), these endocytosis inhibitors showed different levels of inhibition effects. Besides, 4 °C and NaN_3 also displayed strong impact on cellular uptake (down to 15% and 75% respectively), which indicated the uptake of (Bio_2-Chol)Lip was energy-dependent.

The (Bio_2-Chol)Lip uptake in 4T1 and MCF7 cells was shown to be time and concentration dependent (**Fig. S1**). The effect of sodium ions on the rate of (Bio_2-Chol)Lip uptake was delineated by performing the experiment in sodium-free buffer. As shown in **Fig. 7B** and **7D**, a marked decrease (> 45%) in (Bio_2-Chol)Lip uptake was evident in the absence of sodium ions. On the other hand, no significant difference was observed in the uptake when chloride in the incubation buffer was displaced. Hence the uptake process in both the cell lines was found to be highly sodium dependent and chloride independent.

Furthermore, (Bio_2-Chol)Lip uptake was significantly inhibited in the presence of biotin and pantothenic acid which were well known as substrates for SMVT (**Fig. 7B** and **7D**). Interestingly, a significant inhibition in (Bio_2-Chol)Lip uptake was observed in presence of NHS- biotin (devoid of free carboxylic group) and valeric acid (which has free carboxylic group) in 4T1 cell, but no marked inhibition of NHS- biotin in MCF7. Our results correspond to earlier reports suggesting that a free carboxylic group may be essential for specific binding to the

transporter [15]. (Bio_2-Chol)Lip uptake was unaltered in the presence of other structurally unrelated vitamins (ascorbic acid, thiamine). These results along with previous reports suggest that (Bio_2-Chol)Lip internalization in accordance with the characteristics of SMVT transport [15].

In conclusion, all the results indicated that (Bio_2-Chol)Lip could be recognized by sodium-dependent multivitamin transporter (SMVT) on the membrane of breast tumor cells *via* the residues on the surface, and then energy-dependently internalized through a synthetic endocytic pathway including clathrin-mediated, caveolae-mediated and micropinocytosis-mediated endocytosis.

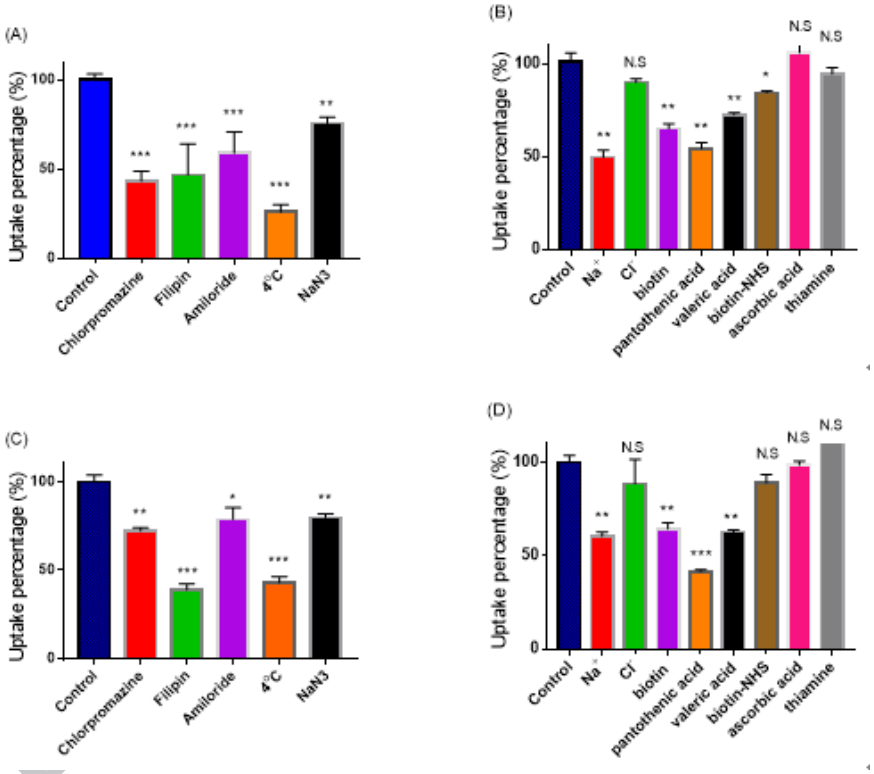

Figure 7. The relative uptake of CFPE-labeled (Bio_2-Chol)Lip on 4T1 cells (A, B) and MCF-7 cells (C, D) for 4h after preincubation of different inhibitors determined by flow cytometer (mean ± SD, *n* =3). *, ** and *** represent $p < 0.05$, $p < 0.01$ and $p < 0.001$ versus control group, respectively, N. S. indicates none significant difference.

3.9. Cytotoxicity

It was demonstrated that cellular uptake of (Bio_2-Chol)Lip was significantly higher than others. To further verify the Bio_2-Chol endowed (Bio_2-Chol)Lip with antiproliferation and the potent active targeting ability of SMVT, *in vitro* cytotoxicity of different liposomes against 4T1 cells and MCF-7 cells was performed by MTT assays.

As shown in **Fig. 8A** and **8C**, free PTX showed higher inhibition rate than PTX-loaded liposomes, because free drugs could be transported into the cells directly and without a drug release process. In addition, according to

the trend of cell viability, PTX-(Bio$_2$-Chol)Lip displayed significant higher inhibition rate than PTX-(Bio-Chol)Lip and PTX-(Bio-Chol)$_2$Lip against 4T1 cells and MCF-7 cells simultaneously. Accordingly, the results suggested that Bio$_2$-Chol could remarkably enhance the cytotoxicity of drug loaded liposomes.

On the other hand, the cytotoxicity of liposomes without drug loaded was also measured. Blank Lip, (Bio-Chol)Lip, (Bio-Chol)$_2$Lip, and (Bio$_2$-Chol)Lip at different concentrations all exhibited little toxicity as the cell viability was more than 89% even at a relatively high concentration, while free PTX solvent (ethanol-cremophor ELP 35 mixture, v/v = 1: 1) displayed an anti-proliferation effect as the concentration increased (**Fig. 8B** and **8D**). Therefore, our liposomal drug delivery systems were safe and nontoxic to be further used *in vivo*.

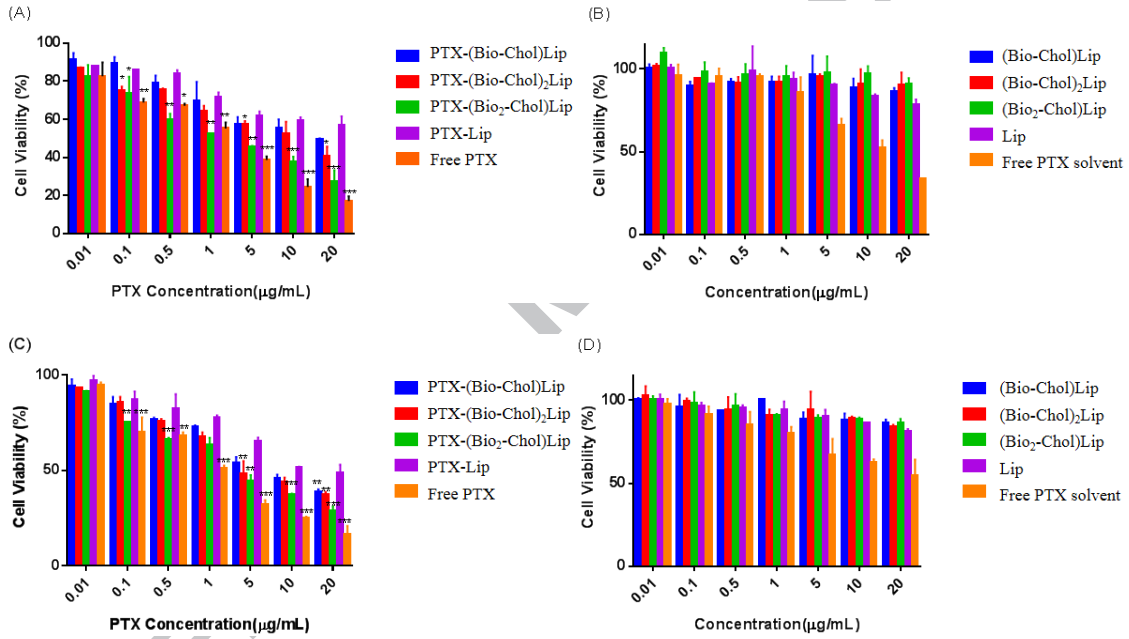

Figure 8. (a) The cytotoxicity study on 4T1 cells (A), MCF-7 cells (C) after treated with various concentrations of PTX-Lip, PTX-(Bio-Chol)Lip, PTX-(Bio-Chol)$_2$Lip, PTX-(Bio$_2$-Chol)Lip and free PTX for 48h (n =3, mean ± SD). (b) The cytotoxicity study on 4T1 cells (B), MCF-7 cells (D) after treated with various concentrations of free PTX solvent, Lip, (Bio-Chol)Lip, (Bio-Chol)$_2$Lip and (Bio$_2$-Chol)Lip for 48h (n =3, mean ± SD). *, ** and *** represent $p < 0.05$, $p < 0.01$ and $p < 0.001$ versus blank Lip group, respectively

Annexin V-FITC/PI apoptosis detection kit was used to study the cell apoptosis induced by PTX-loaded liposomes. As shown in **Fig. 9**, the percentage of apoptosis and necrotic cells was 34.59 ± 3.46% for free PTX, 22.57 ± 1.90% for PTX-Lip, 22.42 ± 3.62% for PTX-(Bio-Chol)Lip, 29.39 ± 2.82% for PTX-(Bio-Chol)$_2$Lip and 35.83 ± 3.00% for PTX-(Bio$_2$-Chol)Lip, respectively. Bio$_2$-Chol modified PTX loaded liposomes and free PTX induced significant stronger cell apoptosis effects, and the results were consistent with the cytotoxicity experiments

in vitro.

What's more, the cytotoxicity and apoptosis study of PTX formations confirmed that (Bio_2-Chol)Lip could remarkably improve the cellular internalization of drug delivery systems, release more therapeutic agents into the cytoplasm and achieve stronger inhibition effect *in vitro*.

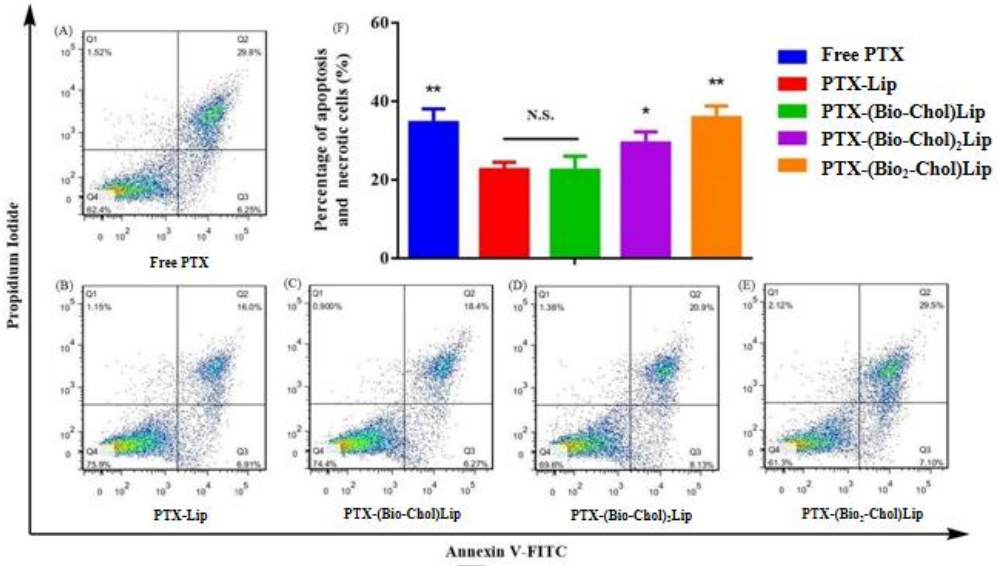

Figure 9. (a) The apoptosis study of 4T1 cells after incubation with free PTX (A), PTX-Lip (B), PTX-(Bio-Chol)Lip (C), PTX-(Bio-Chol)$_2$Lip (D), PTX-(Bio_2-Chol)Lip (E). (b) The percentage of apoptosis and necrotic cells after free PTX and PTX-loaded liposomes treatment (F). *, ** and represent $p < 0.05$, $p < 0.01$ and versus PTX-Lip group, N. S. indicates none significant difference (n =3, mean ± SD).

3.10. Bio-distribution study in plasma and tissues

A perfect delivery system for tail vein administration should have enough circulation time in the bloodstream to reach and diffuse through all tissues and deliver its cargo to the target site. 4T1 tumor-bearing BALB/c mice were used to estimate the plasma distribution of different formulations. We firstly assessed the distribution of the PTX-Lip, PTX-(Bio-Chol)Lip, PTX-(Bio-Chol)$_2$Lip, PTX-(Bio_2-Chol)Lip and free PTX in plasma. The plasma PTX concentration-time profiles were illustrated in **Fig. 10** and the corresponding pharmacokinetic parameters of PTX from different formulations were summarized in Table 2.

It was shown that the area under the concentration-time curve (AUC_{0-t}) of PTX in four types of liposomes were much higher than that of naked PTX within 24h after the same dosage (10 mg/kg) was administrated (Table 2). Meanwhile, PTX-(Bio_2-Chol)Lip could extend the elimination half-life ($t_{1/2}$) of free PTX from 359 min to 601 min ($p < 0.001$) while the smaller-sized particles had longer blood retention [28]. These results suggested that the clearance of PTX in plasma was delayed owing to the sustained release of liposomes. Meanwhile, these data also indicated that all the four types of liposomes showed certain stability which would increase the chance transport to

tumor tissues.

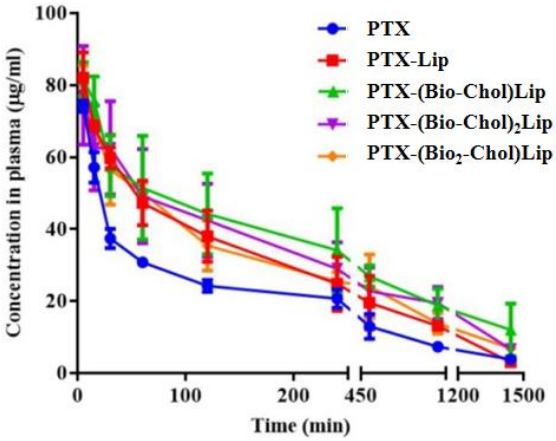

Figure 10. The concentration curve of paclitaxel versus time in plasma after i.v. injection of paclitaxel and PTX-loaded liposomes in mice (n = 3, mean ± SD).

Table 2. Pharmacokinetic parameters of paclitaxel in blood after administration of paclitaxel and liposomes (n =3).

Parameters	$AUC_{(0-t)}$ (g/mL·min)	MRT (min)	T_{max} (min)	C_{max} (μg/mL)	$t_{1/2}$ (min)
Paclitaxel	16360.94 ± 1569.49	340.70 ± 15.46	5	74.17 ± 1.59	358.89 ± 48.86
PTX-Lip	25169.06 ± 1208.74	399.96 ± 22.99	5	82.07 ± 7.02	340.87 ± 46.28
PTX-(Bio-Chol)Lip	35319.11 ± 8067.41	500.99 ± 62.67	5	81.66 ± 4.73	729.22 ± 529.13
PTX-(Bio-Chol)$_2$Lip	31447.98 ± 6352.58	470.13 ± 21.04	5	77.14 ± 13.69	536.38 ± 154.64
PTX-(Bio$_2$-Chol)Lip	27872.99 ± 1585.19	458.93 ± 3.88	5	80.29 ± 5.08	600.68 ± 217.75

To further evaluate the breast tumor targeting capability of formulations, the distribution of liposomes in various organs and tumor tissues were also studied in 4T1 tumor-bearing BALB/c mice.

As shown in **Fig. 11** and Table 3, it was clearly observed that the PTX of PTX-(Bio$_2$-Chol)Lip accumulated more than other groups in the breast tumor from 15 min to 1440 min after administration (21985.38 ± 993.94 μg/g·h, **Fig. 11**), displaying the strongest breast tumor targeting ability of PTX-(Bio$_2$-Chol)Lip.

PTX-loaded liposomes and naked PTX all reached the maximum distribution in the breast tumor at 480 min after injection. Especially, the relative absorption efficiency (REs) of PTX-(Bio$_2$-Chol)Lip reached 5.61 times ($p < 0.001$) that of PTX, the concentration efficiencies (CEs) were also enhanced to 5.06 times ($p < 0.001$). These findings showed that PTX-(Bio$_2$-Chol)Lip had a higher affinity for SMVT on breast tumor, enabling more PTX to be transported to targeted tissues with minimal side effect. All these results suggested that PTX-(Bio$_2$-Chol)Lip had the potential as breast tumor targeting carriers for hydrophobic anticancer agents.

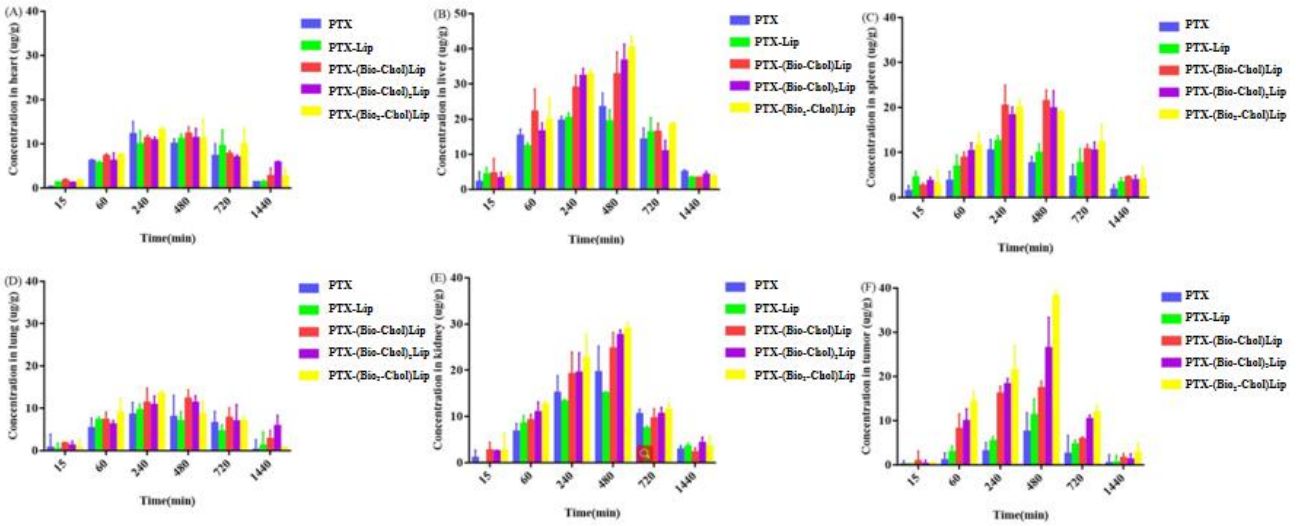

Figure 11. *In vivo* distribution of 4T1-tumor bearing mice at different time points after i.v. injection of paclitaxel and PTX-loaded liposomes in mice, including heart (A), liver (B), spleen (C), lung (D), kidney (E) and tumor (F). Data represent mean±SD. (n = 3, mean ± SD).

Table 3. Pharmacokinetic parameters of paclitaxel in tumor tissues after administration of paclitaxel and liposomes (*n* =3).

Parameters	$AUC_{(0-t)}$ (μg/g·min)	MRT (min)	T_{max} (min)	C_{max} (μg/g)	RE	CE
Paclitaxel	3920.90 ± 140.91	533.07 ± 55.59	480	7.54 ± 0.77	-	-
PTX-Lip	6779.30 ± 720.60	556.63 ± 4.79	480	11.30 ± 2.56	1.73	1.50
PTX-(Bio-Chol)Lip	11888.57 ± 150.29	479.12 ± 10.83	480	17.36 ± 1.11	3.03	2.30
PTX-$(Bio\text{-}Chol)_2$Lip	15867.44 ± 189.01	504.30 ± 5.86	480	22.57 ± 1.81	4.05	3.00
PTX-(Bio_2-Chol)Lip	21985.38 ± 993.94	507.30 ± 31.38	480	38.16 ± 0.82	5.61	5.06

3.11. In vivo imaging

To investigate the *in vivo* targeting efficiency and monitoring the accumulation behavior in breast tumor site, DiD-labeled liposomes were employed. As shown in **Fig. 12**, images *in vivo* indicated that PTX-(Bio_2-Chol)Lip presented the highest fluorescence intensity and the best accumulation in tumor region from 1h to 24h in contrast to other liposomes after systemic administration. The four types of liposomes showed weak fluorescence signal at tumor site 2h later, and the fluorescence intensity reached its maximum at 8h which was in accordance with the results of bio-distribution. These results displayed the strongest breast tumor targeting capability of (Bio_2-Chol)Lip.

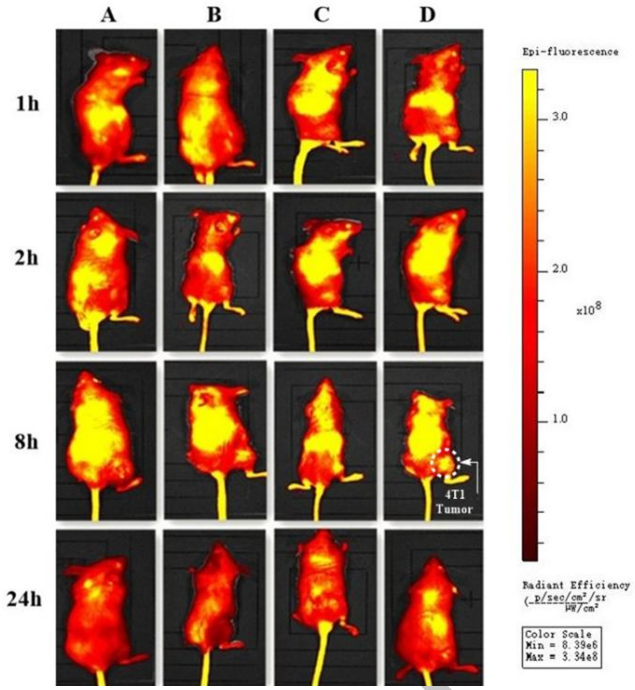

Figure 12. *In vivo* images of 4T1-tumor bearing mice at different time points after systemic administration of DiD-loaded liposomes. A: DiD-Lip, B: DiD-(Bio-Chol)Lip, C: DiD-(Bio-Chol)$_2$Lip, D: DiD-(Bio$_2$-Chol)Lip (n =4).

These bio-distribution and *in vivo* imaging results further proved that PTX-(Bio$_2$-Chol)Lip possessed a high selective breast tumor transporting ability not only *in vitro* but also *in vivo*. Hence, PTX-(Bio$_2$-Chol)Lip could be superior to other groups in the therapeutic efficacy of breast cancer.

4. Conclusion

In conclusion, we have successfully designed and developed a series of biotin modified liposomes as active targeting drug delivery systems for the therapy of breast cancers. In particular, we broke the traditional design concept of using single branched ligands to modify liposomes and prepared the double branched biotin modified liposome for the first time. Excitingly, in the *in vitro* uptake and *in vivo* distribution experiments, the double branched biotin modified liposome ((Bio$_2$-Chol)Lip) exhibited excellent targeting ability of breast cancer. In contrast, SMVT negative expressed cells have very little uptake of (Bio$_2$-Chol)Lip, thus ensuring very low systemic toxicity. In addition, cytotoxicity and apoptosis assays showed that PTX-(Bio$_2$-Chol)Lip exhibited better therapeutic effects for breast cancer than other PTX-loaded liposomes. All these results indicate that increasing the density of ligand on the surface of liposomes can significantly improve tumor targeting ability of liposomes. Especially, the modification of cholesterol by double branched ligands can further improve the active targeting of liposomes while keeping the dosage of cholesterol low. We believe that the strategy of modifying cholesterol with

multi-branched ligands will open a novel and exciting chapter in the design of tumor-specific diagnostic reagents and active targeting drug delivery systems.

Acknowledgement

This work was supported by the National Natural Science Foundation of China (No. 81573286, No. 81773577 & No. 21472130), the Sichuan Science and Technology Program (2018JY0537) and the Fundamental Research Funds for the Central Universities (2012017yjsy211).

Conflict of Interest

The authors declare no competing financial interest.

Appendix A. Supporting Information

Supplementary data associated with this article can be found in the online version at.

References

[1] S.S.S. Pindiprolu, P.T. Krishnamurthy, P.K. Chintamaneni, Pharmacological targets of breast cancer stem cells: a review, N-S. Arch. Pharmacol. 391 (2018) 463-479.

[2] J. Ferlay, C. Héry, P. Autier, R. Sankaranarayanan, Global burden of breast cancer. In: Li C (ed) Breast cancer epidemiology. Springer, New York, (2010).

[3] a) X. Sun, S. Qin, C. Fan, C. Xu, N. Du, H. Ren, Let-7: a regulator of the ERalpha signaling pathway in human breast tumors and breast cancer stem cells, Oncol. Rep. 29 (2013) 2079-2087; b) H.S. Kim, V-H. Hoang, M. Hong, K.C. Kim, J. Ann, C-T. Nguyen, J.H. Seo, H. Choi, J.Y. Kim, K-W. Kim, W.S. Byun, S. Lee, S. Lee, Y-G. Suh, J. Chen, H-J. Park, T-M. Chod, J.Y. Kim, J. Lee, Investigation of B,C-ring truncated deguelin derivatives as heat shock protein 90 (HSP90) inhibitors for use as anti-breast cancer agents, Bioorg. Med. Chem. 27 (2019) 1370-1381; c) O.M. Abdelhafez, E.Y. Ahmed, N.A.A. Latif, R.K. Arafa, Z.Y.A. Elmageed, H.I.Ali, Design and molecular modeling of novel P38α MAPK inhibitors targeting breast cancer, synthesized from oxygen heterocyclic natural compounds, Bioorg. Med. Chem. 27 (2019) 1308-1319; d) A. Monastyrskyi, N. Nilchan, V. Quereda, Y. Noguchi, C. Ruiz, W. Grant, M. Cameron, D. Duckett, W. Roush, Development of dual casein kinase 1δ/1ε (CK1δ/ε) inhibitors for treatment of breast cancer, Bioorg. Med. Chem. 26 (2018) 590-602; e) S. Dutta, O.L. Charcas, S. Tanner, F. Gradek, V. Driffort, S. Roger, K. Selander, S.E. Velu, W. Brouillette, Discovery and evaluation of nNav1.5 sodium channel blockers with potent cell invasion inhibitory activity in

breast cancer cells, Bioorg. Med. Chem. 26 (2018) 2428-2436; f) R.Z. Batran, A.F. Kassem, E.M.H. Abbas, S.A. Elseginy, M.M. Mounier, Design, synthesis and molecular modeling of new 4-phenylcoumarin derivatives as tubulin polymerization inhibitors targeting MCF-7 breast cancer cells, Bioorg. Med. Chem. 12 (2018) 3474-3490; g) Y. Sugimoto, D.B. Sawant, H.A. Fisk, L. Mao, C. Li, S. Chettiar, P-K. Li, M.V. Darby, R.W. Brueggemeier, Novel pyrrolopyrimidines as Mps1/TTK kinase inhibitors for breast cancer, Bioorg. Med. Chem. 25 (2017) 2156-2166.

[4] R. Mahato, W.Y. Tai, K. Cheng, Prodrugs for Improving Tumor Targetability and Efficiency, Adv. Drug. Deliv. Rev. 63 (2011) 659-670.

[5] a) C-S. Lee, H. Kim, J. Yu, S.H. Yu, S. Ban, S. Oh, D.J. Jeong, J. Im, M.J. Baek, T.H. Kim, Doxorubicin-loaded oligonucleotide conjugated gold nanoparticles: A promising in vivo drug delivery system for colorectal cancer therapy, Eur. J. Med. Chem. 142 (2017) 416-423; b) V.L. Joncour, P. Laakkonen, Seek & Destroy, use of targeting peptides for cancer detection and drug delivery, Bioorg. Med. Chem. 26 (2018) 2797-2806.

[6] F.H. Nasr, S. Khoee, Design, characterization and in vitro evaluation of novel shell crosslinked poly(butylene adipate)-co-N-succinyl chitosan nanogels containing loteprednol etabonate: A new system for therapeutic effect enhancement via controlled drug delivery, Eur. J. Med. Chem. 102 (2015) 132-142.

[7] C.L. Zhuang, X.H. Guan, H. Ma, H. Cong, W.N. Zhang, Z.Y. Miao, Small molecule-drug conjugates: A novel strategy for cancer-targeted treatment, Eur. J. Med. Chem. 163 (2019) 883-895.

[8] Y. Zhang, H.K. Deng, H.F. Zhou, Y.C. Lu, L.C. Shan, S.M-Y. Lee, G.Z. Cui, A novel agent attenuates cardiotoxicity and improves antitumor activity of doxorubicin in breast cancer cells, J. Cell. Biochem. 120 (2019) 5913-5922.

[9] P. Pathak, V. Dhawan, A. Magarkar, R. Danne, S. Govindarajan, S. Ghosh, F. Steiniger, P. Chaudhari, V. Gopal, A. Bunker, T. Róg, A. Fahr, M. Nagarsenker, Design of cholesterol arabinogalactan anchored liposomes for asialoglycoprotein receptor mediated targeting to hepatocellular carcinoma: In silico modeling, in vitro and in vivo evaluation, Int. J. Pharm. 509 (2016) 149-158.

[10] Y. Tian, J. Xia, L. Zhang, J. Zhang, Y. Jiang, Y. Zhang, L. Yang, Q. Zhang, L. Xia, Ionic liquid based polymeric liposomes: A stable and biocompatible soft platform for bioelectrochemistry, Bioelectrochemistry. 111 (2016) 41-48.

[11] Y. Zhao, J. Zhu, H. Zhou, X. Guo, T. Tian, S. Cui, Y. Zhen, S. Zhang, Y. Xu, Sucrose ester based cationic liposomes as effective non-viral gene vectors for gene delivery, Colloids. Surf, B. 145 (2016) 454-461.

[12] S. Saha1, R. Majumdar, A. Hussain, R.R. Dighe, A.R. Chakravarty, Biotin-conjugated tumour-targeting

photocytotoxic iron(III) complexes, P. Roy. Soc. A-Math. Phy. 371 (2013) 20120190/1-20120190/15.

[13] a) G. Tripodo, D. Mandracchia, S. Collina, M. Rui, D. Rossi, New Perspectives in Cancer Therapy: The Biotin-Antitumor Molecule Conjugates, Med. Chem, S1 (2014) 1-8; b) Ł. Uram, M. Szuster, A. Filipowicz, M. Zaręba, E. Wałajtys-Rode, S. Wołowie, Cellular uptake of glucoheptoamidated poly(amidoamine) PAMAM G3 dendrimer with amide-conjugated biotin, a potential carrier of anticancer drugs, Bioorg. Med. Chem. 25 (2017) 706-713.

[14] R. Rodriguez-Melendez, J. Zempleni, Regulation of gene expression by biotin (review), J. Nutr. Biochem. 14 (2003) 680-690.

[15] A.D. Vadlapudi, R.K. Vadlapatla, D. Pal, A.K. Mitra, Biotin uptake by T47D breast cancer cells: Functional and molecular evidence of sodium-dependent multivitamin transporter (SMVT), Int. J. Pharm. 441 (2013) 535-543.

[16] W.X. Ren, J.Y. Han, S. Uhm, Y.J. Jang, C. Kang, J-H. Kim, J.S. Kim, Recent development of biotin conjugation in biological imaging, sensing, and target delivery, Chem. Commun., 51 (2015) 10403-10418.

[17] X. Tian, H.Z. Yin, S.C. Zhang, Y. Luo, K. Xu, P. Ma, C.G. Sui, F.D. Meng, Y.P. Liu, Y.H. Jiang, J. Fang, Bufalin loaded biotinylated chitosan nanoparticles: An efficient drug delivery system for targeted chemotherapy against breast carcinoma, Eur. J. Pharm. Biopha. 87 (2014) 445-453.

[18] Y.H. Bae, K. Park, Targeted drug delivery to tumors: myths, reality and possibility, J. Control. Release. 153 (2011) 198-205.

[19] a) A. Pratesi, M. Ginanneschi, F. Melani, M. Chinol, A. Carollo, G. Paganelli, M. Lumini, M. Bartoli, M. Frediani, L. Rosi, G. Petrucci, L. Messorib, A.M. Papini, Design and solid phase synthesis of new DOTA conjugated (+)-biotin dimers planned to develop molecular weight-tuned avidin oligomers, Org. Biomol. Chem. 13 (2015) 3988-4001; b) D.S. Wilbur, S.I. Park, M.K. Chyan, F. Wan, D.K. Hamlin, J. Shenoi, Y. Lin, S.M. Wilbur, F. Buchegger, A. Pantelias, J.M. Pagel, O.W. Press, Design and Synthesis of Bis-Biotin-Containing Reagents for Applications Utilizing Monoclonal Antibody-Based Pretargeting Systems with Streptavidin Mutants, Bioconjugate Chem. 21 (2010) 1225-1238; c) K.J. Hamblett, O.W. Press, D.L. Meyer, D.K. Hamlin, D. Axworthy, D.S. Wilbur, P.S. Stayton, Role of Biotin-Binding Affinity in Streptavidin-Based Pretargeted Radioimmunotherapy of Lymphoma, Bioconjugate Chem. 16 (2005) 131-138; d) L. Correa-González, C.A. de Murphy, G. Ferro-Flores, M. Pedraza-López, E. Murphy-Stack, D. Mino-León, G. Pérez-Villasenor, Y. Díaz-Torres, R. Muóz-Olvera, Uptake of ^{153}Sm-DTPA-bis-biotin and ^{99m}Tc-DTPA-bis-biotin in rat AS-30D-hepatoma cells, Nucl. Med. Biol. 30 (2003) 135-140.

[20] a) M-W. Louie, M.H-C. Lam, K.K-W. Lo, Luminescent Polypyridinerhenium(I) Bis-Biotin Complexes as Crosslinkers for Avidin, Eur. J. Inorg. Chem. 2009 (2009) 4265-4273; b) K.K-W Lo, J. S-Y. Lau, Cyclometalated Iridium(III) Diimine Bis(biotin) Complexes as the First Luminescent Biotin-Based Cross-Linkers for Avidin, Inorg. Chem. 46 (2007) 700-709.

[21] X. Li, B. Qu, X. Jin, L. Hai, Y. Wu, Design, synthesis and biological evaluation for docetaxel-loaded brain targeting liposome with "lock-in" function, J. drug. Target. 22 (2014) 251-261.

[22] Y. Peng, Y. Zhao, Y. Chen, Z.Z. Yang, L. Zhang, W.J. Xiao, J.C. Yang, L. Guo, Y. Wu, Dual-targeting for brain-specific liposomes drug delivery system: Synthesis and preliminary evaluation, Bioorg. Med. Chem. 26 (2018) 4677-4686.

[23] K.R. Shi, J.P. Li, Z.L. Cao, P. Yang, Y. Qiu, B. Yang, Y. Wang, Y. Long, Y.Y. Liu, Q.Y. Zhang, J. Qian, Z.R. Zhang, H.L. Gao, Q. He, A pH-responsive cell-penetrating peptide-modified liposomes with active recognizing of integrin $\alpha_v\beta_3$ for the treatment of melanoma, J. Control. Release. 217 (2015) 138-150.

[24] S. Rojas, J.D. Gispert, R. Martín, S. Abad, C. Menchón, D. Pareto, Biodistribution of amino-functionalized diamond nanoparticles. In vivo studies based on 18F radionuclide emission, ACS Nano. 5 (2011) 5552-5559.

[25] B. Jang, J-Y. Park, C-H. Tung, I-H. Kim, Y. Choi, Gold nanorod-photosensitizer complex for near-infrared fluorescence imaging and photodynamic/photothermal therapy in vivo. ACS Nano. 5 (2011) 1086-1094.

[26] G. Sharma, A. Modgil, B. Layek, K. Arora, C. Sun, B. Law, J. Singh, Cell penetrating peptide tethered bi-ligand liposomes for delivery to brain in vivo: biodistribution and transfection, J. Control. Release. 167 (2013) 1-10.

[27] S.M. Noh, M.O. Park, G. Shim, S.E. Han, H.Y. Lee, J.H. Huh, Pegylated poly-l-arginine derivatives of chitosan for effective delivery of siRNA, J. Control. Release. 145 (2010) 159-164.

[28] Y.Y. Liu, R. Ran, J.T. Chen, Q.F. Kuang, J. Tang, L. Mei, Q.Y. Zhang, H.L. Gao, Z.Y. Zhang, Q. He, Paclitaxel loaded liposomes decorated with a multifunctional tandem peptide for glioma targeting, Biomaterials. 35 (2014) 4835-4847.